INVESTIGATION OF VOLUME RECOMBINATION IN A CESIUM PLASMA

Yu. M. ALESKOVSKIĬ

Moscow State University

Submitted to JETP editor October 2, 1962

J. Exptl. Theoret. Phys. (U.S.S.R.) **44**, 840-847 (March, 1963)

Probe and spectrometric determinations of the recombination coefficient α and electron temperature T_e are performed for a decaying cesium plasma. No dependence of α on pressure has been found in the range $p = 5 \times 10^{-3} - 10^{-1}$ mm Hg. An analysis of the results reveals that recombination occurs in the triple collision of two electrons and an ion. An important role in the recombination mechanism is played by radiative cascading due to collisions of the second kind. The recombination coefficient computed for a plasma with density $10^{11} - 10^{14}$ cm^{-3} and $T_e = 0.1 - 0.3$ eV agrees satisfactorily with experimental results.

THE investigation reported here was performed to determine the recombination rate of cesium plasma and to discover the principal type of elementary recombination process in relatively weakly ionized cesium (< 20%). Table I summarizes the literature regarding recombination in cesium. Here p is the cesium vapor pressure, n_e is the electron and ion concentration, and T_e is the electron temperature. The recombination coefficient α is given by

$$dn_e/dt = -\alpha n_e^2. \quad (1)$$

The inconsistency of these data and the lack of a sufficiently clear understanding of the recombination mechanism induced the present investigation.

1. EXPERIMENTAL TECHNIQUE

The measurements were performed in a decaying plasma following current cutoff in a cylindrical discharge tube 15 cm long and of radius R = 1.3 cm, using both an electric probe and spectroscopy. By continuous evacuation the residual gas pressure was maintained < 10^{-6} mm. The cesium vapor pressure was determined from the temperature of a branch tube containing liquid metal; the main tube was raised to a higher temperature in an electric furnace. The low-voltage arc in the cesium vapor lasted ~5 μsec, with the current changing from 1 to 10 A. The electric circuit provided for arc extinction by triggering a bypass thyratron and by removing the potential from the discharge tube during the entire deionization time. The work was performed at 50 cps.

When a plasma is being deionized, especially at low pressures, volume recombination is accompanied by charge diffusion to the tube walls. In order to exclude this source of losses a strong homogeneous magnetic field parallel to the tube axis was applied to the plasma. Preliminary studies showed that under our conditions diffusion is suppressed at H ~ 1 - 1.5 kOe. At p ≥ 0.1 mm

Table I

Experimental conditions			Experimental method	α, cm^3/sec
p, mm Hg	$10^{-11}n_e$, cm^{-3}	T_e, eV		
0.01--0.11	8	0.1	Probe and optical measurements in afterglow	$3.5 \cdot 10^{-10}$[1]*
0.68--2.6	—	—	Microwave and optical measurements in afterglow	$3.5 \cdot 10^{-7}$ —$1.4 \cdot 10^{-6}$[2]**
10^{-5}--10^{-6}	5	0.2	Probe measurements in thermally ionized plasma	~$(1-2) \cdot 10^{-10}$[3]***
10^{-5}--10^{-6}	40	0.19	Probe measurements in thermally ionized plasma	≤$3 \cdot 10^{-11}$[4]***

*No clear α-f(p) relationship was observed; the recombination mechanism was not established.

**Dissipative recombination is assumed.

***It is assumed that recombination occurs in triple collisions: two electrons + ion.

volume recombination predominates even in the absence of a magnetic field.

From an oscillographic record of the ion current to a negative cylindrical probe (5 cm long and 0.02 cm in diameter) and a computation of charge concentration n_e using Bohm's formula,[5] the relaxation time τ for recombination of charges and the recombination coefficient α are determined:

$$\frac{1}{\tau} = \frac{1}{n_e}\frac{dn_e}{dt}, \qquad \alpha = \frac{1}{n_e\tau}. \tag{2}$$

For spectroscopic measurements radiation from the discharge tube was projected perpendicular to the tube axis into the slit of an UM-2 monochromator. Visible radiation was registered by a FÉU-17 photomultiplier, and infrared radiation by a FEU-22 photomultiplier. Signals from the photomultipliers were fed to a cathode follower before being recorded by an oscillograph. A standard temperature-calibrated tungsten ribbon lamp was used to calibrate the optical channel in absolute radiation units.

2. RESULTS

Figure 1 shows typical curves representing the variation of plasma concentration and electron temperature in the afterglow. The temperature T_e was determined spectroscopically from the intensity distribution in the 6P electron continuum by means of data in [6]. Sufficiently reliable measurements can be obtained in this way early in the afterglow (up to 200–300 μsec), since the intensity in the "tail" of the band drops rapidly to a very small level. The relative change of T_e later in the afterglow was obtained from probe measurements of the ion current i_p and from the intensity I of the band head. The first of these quantities was determined from Bohm's formula

$$i_p = 0.4Sn_e\sqrt{\frac{2kT_e}{m_p}}, \tag{3}$$

where S is the collecting surface of the probe and m_p is the ion mass; the second quantity is given by [6]

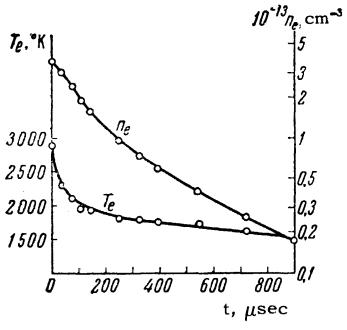

FIG. 1. Variation of plasma concentration n_e and electron temperature T_e during deionization. p = 5 × 10^{-3} mm. H = 1300 Oe.

Table II

p, mm Hg	$10^{-13}n_e$, cm^{-3}	T_e, eV	$10^4\tau$, sec	$10^{10}\alpha$, cm^3/sec
$5\cdot10^{-3}$	3.7	0.25	2.1	1.29
	3.1	0.2	1.65	1.95
	1.6	0.17	1.8	3.5
	0.75	0.16	3.15	4.23
	0.40	0.15	3.85	6.5
$1.5\cdot10^{-2}$	2.7	0.24	1.8	2.0
	1.7	0.17	2.4	2.5
	0.89	0.14	3.5	3.2
	0.55	0.13	5.35	3.4
10^{-1}	5.9	0.26	1.25	1.36
	1.7	0.15	2.2	2.82
	0.40	0.13	4.4	5.7
	0.55	0.12	2.2	8.27
	0.14	0.11	6.5	11

$$I = 1.07\cdot10^{-22}n_e^2T_e^{-3/2}. \tag{4}$$

Hence the ratio

$$\frac{i_p^2}{I} \sim T_e^{5/2} \tag{5}$$

is independent of n_e and is quite sensitive to temperature changes.

Table II gives several values of τ and α calculated from the deionization curves $n_e(t)$. Even with a twenty-fold pressure difference, for close values of n_e and T_e the values of τ do not differ appreciably; this provides evidence of the recombination character of the deionization.

Optical observations show the existence of two kinds of recombination radiation in a decaying plasma; these are the continuum mentioned above and the lines of the diffuse and fundamental series 6P – nD and 5D – nF. The continuous spectrum decreases from its maximum at the instant when the discharge is cut off, with a time constant approximately equal to $\tau/2$ for the head of the band. Figure 2 shows oscillograms of two wavelengths of the 6P band. The lines behave entirely differently in the afterglow; immediately after the termination of the discharge their intensity drops quickly and then begins to rise, reaching a maximum after a

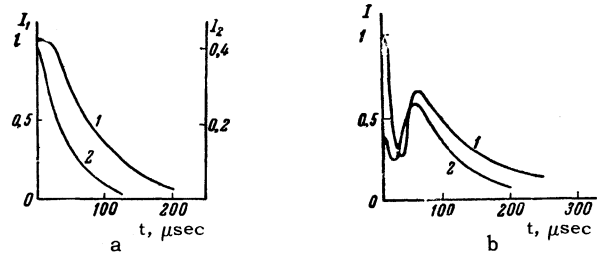

FIG. 2. Variation of radiation intensity in afterglow (p = 8 × 10^{-3} mm, H = 0). a – electron continuum 6P (1 – λ = 4935 Å; 2 – λ = 4480 Å); b – line spectrum (1 – $6P_{3/2} - 8D_{3/2}$; 2 – $6P_{3/2} - 14D_{3/2,5/2}$).

Table III.

λ, Å	Transition	$E/h\nu$, cm^{-1}
10124.1—10025.4	$5D - 4F$	$2.12 \cdot 10^{13}$
9208.4—9172.4	$6P_{3/2} - 6D_{3/2,5/2}$	$7.1 \cdot 10^{12}$
8761.4	$6P_{1/2} - 6D_{3/2}$	$2.84 \cdot 10^{12}$
8081.2—8001.8	$5D - 5F$	$1.7 \cdot 10^{12}$
7281.1—7230.5	$5D - 6F$	$6.65 \cdot 10^{11}$
6985.4—6975.2	$6P_{3/2} - 7D_{3/2,5/2}$	$1.23 \cdot 10^{12}$
6872.3—6826.5	$5D - 7F$	$3.8 \cdot 10^{11}$
6725.1	$6P_{1/2} - 7D_{3/2}$	$8.5 \cdot 10^{11}$
6630.5—6587.8	$5D - 8F$	$2.4 \cdot 10^{11}$
6474.4—6433.7	$5D - 9F$	$1.5 \cdot 10^{11}$
6367.3—6327.1	$5D - 10F$	$7.7 \cdot 10^{10}$
6219.3—6214.8	$6P_{3/2} - 8D_{3/2,5/2}$	$3.94 \cdot 10^{11}$
6012.1	$6P_{1/2} - 8D_{3/2}$	$2.0 \cdot 10^{11}$
5849.1—5846.1	$6P_{3/2} - 9D_{3/2,5/2}$	$1.35 \cdot 10^{11}$
5665.5	$6P_{1/2} - 9D_{3/2}$	$5.55 \cdot 10^{10}$
5638.2—5637.3	$6P_{3/2} - 10D_{3/2,5/2}$	$4.25 \cdot 10^{10}$
5505.3—5504.3	$6P_{3/2} - 11D_{3/2,5/2}$	$2.3 \cdot 10^{10}$
5465.2	$6P_{1/2} - 10D_{3/2}$	$2.6 \cdot 10^{10}$
5415.7—5414.5	$6P_{3/2} - 12D_{3/2,5/2}$	$1.0 \cdot 10^{10}$
5352.2—5351.7	$6P_{1/2} - 11D_{3/2}$	$1.7 \cdot 10^{10}$
5342.4	$6P_{3/2} - 13D_{3/2,5/2}$	
5305.6—5305.2	$6P_{3/2} - 14D_{3/2,5/2}$	$5.8 \cdot 10^{9}$
5270.2—5270.0	$6P_{3/2} - 15D_{3/2,5/2}$	$6.9 \cdot 10^{9}$
5257.1	$6P_{1/2} - 12D_{3/2}$	
5000—4000	6P continuum	$\int \frac{E_\nu d\nu}{h\nu} = 4.0 \cdot 10^{10}$
		$\sum \frac{E}{h\nu} = 3.71 \cdot 10^{13}$

few tens of microseconds (Fig. 2b). Similar behavior of the lines in the afterglow was previously observed in other gases.[7-9] The time required to reach the second maximum is reduced as the initial concentration n_e, pressure p, and magnetic field H increase.

We measured the energy E radiated per cm of tube length during the entire time of the afterglow in the continuum and in lines within the interval 4000—10 000 Å. Table III gives the ratio $E/h\nu$ representing the number of photons or, equivalently, recombination acts accompanied by emission of the corresponding line. Here $p = 8 \times 10^{-3}$ mm, H = 1300 Oe, $T_{e0} = 2750°K$, and $n_{e0} = 3.9 \times 10^{13}$ cm^{-3}. In order to compute the initial number N_{e0} of ions per unit length of the tube, the radial distribution of ions must be known as well as the axial concentration n_e. Therefore the intensity distribution I(x) for the head of the continuum was measured in the tube cross section; then the method described in [9] was used to calculate the radial distribution I(r) of the column. Using (4), $n_e(r)$ can be determined for the purpose of calculating

$$N_{e0} = 2\pi \int_0^R n_e(r)\, r dr.$$

The result $N_{e0} = 8.8 \times 10^{13}$ cm^{-1} indicates that about half of the charged undergo radiative recombination (Table III).

3. DISCUSSION OF RESULTS

Table II shows that the recombination coefficient is practically independent of pressure but increases rapidly as the electron temperature is reduced. This casts doubt on Loeb's assertion that molecular ions participate in recombination in cesium at low pressures. Indeed, if, following Loeb, it is assumed that the recombination rate is given by the rate of molecular ion formation in triple collisions $Cs^+ + 2Cs \rightarrow Cs_2^+ + Cs$ and the frequency of this process is taken as $z = 10^5 p^2$/sec, [10] the recombination coefficient with the dissociation $Cs_2^+ + e \rightarrow 2Cs$ will be $\alpha' = 10^5 p^2/n_e$ and should increase with the pressure. For $p = 5 \times 10^{-3}$ mm and $n_e = 3.7 \times 10^{13}$ cm^{-3} the result $\alpha' \approx 7 \times 10^{-14}$ cm^3/sec obtained from the given formula is several orders of magnitude smaller than the observed value. Moreover, when a molecule dissociates excited atoms can be formed only in states having ionization energies $V_i \geq V_d$, where the molecular-ion dissociation energy is $V_d = 0.45$ eV, [11] i.e., transitions from levels above 8D should not be observed in the afterglow.

The different behaviors of the line spectrum and continuous spectrum in the afterglow (Fig. 2) indicate the existence of two different recombination processes. The energy emitted in discrete lines is almost three orders of magnitude greater than in the continuum (Table III); therefore re-

combination in the two-body collision $Cs^+ + e \rightarrow Cs + h\nu_R$ does not play an important part under our experimental conditions.

It can be assumed that in our case, as in [3,4], three-body recombination into excited levels ($Cs^+ + 2e \rightarrow Cs^* + e$) occurs, as suggested recently by D'Angelo [12] to account for the observed large values of recombination coefficients. The population of excited states calculated by D'Angelo's method for low-lying levels (4F and 6D) is 20—25 times smaller than the experimental result (Table IV). The difference is insignificant for high levels. In these calculations transition probabilities calculated from the tables in [13] and the relative transition probabilities of the series 6P – nD in [14] were used. The recombination coefficient calculated by D'Angelo's method [12] is 40 times smaller than our measured value. This result suggests that a large contribution to the population of lower-lying levels and therefore to the recombination coefficient is attributable to radiative cascading from higher states as a result of electron collisions of the second kind.

Table IV. Population of excited CsI states, $N(10^8\ cm^{-3})$ ($T_e = 2750°\ K$, $n_e = 3.9 \times 10^{13}\ cm^{-3}$)

State	Experiment	Calculated by D'Angelo's method	Calculated with account of radiative cascading
6D	63	3.1	70.5
4F	31	1.2	37.5
7D	9.2	2.26	
5F	10	1.9	
8D	3.0	1.3	
9D	1.6	0.90	

We thus have the following general scheme for the recombination process. Electrons are captured into excited states through triple collisions of two electrons and an ion. However, this does not end the recombination process. An electron can go to a lower level, either spontaneously or through a collision of the second kind, or to a higher level of the continuum through a collision of the first kind. All these processes determine the populations of excited atomic states. Denoting by A_{if} and ${}^iC_f$, respectively, the probabilities of spontaneous and collisional transitions $i \rightarrow j$, and by N_i the population of level i, the rate of ground-state transitions (the recombination rate [1]) is described by

$$\frac{dn_e}{dt} = -\sum_{i=2}^{\infty}[A_{i1}N_i + {}^iC_1 n_e N_i] = -\alpha n_e^2 \qquad (6)$$

from which the recombination coefficient is determined. The level populations N_i must, of course, be determined in advance. Calculations of this kind have recently been performed for hydrogen. [15, 16]

4. CALCULATION OF THE RECOMBINATION COEFFICIENT

In the present case the calculation is considerably simplified if it is noted that the principal contribution comes from 5D – 4F and 6P – 6D transitions (Table III). Recombination can be regarded as concluded herewith since the probability of excitation and ionization of deep 5D and 6P levels at low temperatures of a decaying plasma is negligibly small. The problem is therefore reduced to calculating the populations of 4F and 6D levels, which determine the recombination coefficient according to (6).

In a quasi-stationary state the number of transitions contributing to the population n of a level equals the number of transitions from the level. A simple estimate shows that for $n_e > 10^{11}\ cm^{-3}$ the characteristic time required to establish any state does not exceed 1 μsec, which is at least two orders of magnitude smaller than the deionization time of the plasma. The system of balance equations is written for low-lying levels from n = 4 to n = 15. For higher values of n the population can be regarded as in equilibrium with the electron continuum and as determinable from Saha's equation. For each value of n only states with the largest value of $l = n - 1$ are considered, since the remaining sublevels make a much smaller contribution. In the balance equation of state i the following processes are taken into account: (1) electron capture from the continuum in a triple collision, (2) collisional and spontaneous transitions from higher quantum states, (3) excitation from a lower state, (4) ionization by electron collision, (5) collisional and spontaneous transitions to a lower state, and (6) a collisional transition to a higher quantum state. Only transitions between neighboring states ($\Delta n = \pm 1$) are taken into account. It is also necessary to determine the coefficients of the equations. For the ionization probability P_i the classical Thomson cross section was used; an average over a Maxwellian distribution yielded

$$P_i = 5.4T_e^{-3/2} \exp(-V_i/kT_e)\, K_i. \qquad (7)$$

Here V_i is ionization potential of level i, and

[1] Although recombination does not occur here through a two-body collision, for convenient comparison with the literature we shall continue to use Eq. (1).

$$K_l \approx (kT_e/V_l)^2 \text{ for } (V_l/kT_e) > 1,$$

$$K_l \approx (kT_e/V_l) \text{ for } (V_l/kT_e) < 1.$$

The probability β_i of triple recombination is related to P_i by the principle of detailed balancing. We obtain

$$\beta_i = 1.12 \cdot 10^{-15} \cdot g_i T_e^{-3} K_i, \quad (8)$$

where g_i is the statistical weight of the level.

For the probabilities of inelastic collisions of the first and second kinds in transitions between various levels, ${}_iC^k$ and ${}^iC_j$, cross sections from Allen's book [17] were used; after averaging we have

$${}_iC^k = 2.43 \cdot 10^{-7} A_{ki} \frac{g_k}{g_i} \lambda^2 T_e^{-3/2} K_{ik} \exp(-V_{ik}/kT_e), \quad (9)$$

$${}^iC_j = 2.43 \cdot 10^{-7} A_{ij} \lambda^2 T_e^{-3/2} K_{ij}, \quad (10)$$

where λ is given in microns.

The lack of data regarding the probabilities of transitions between states with large values of l made it necessary to perform suitable calculations using the semi-empirical method of Petrashen' and Abramenkov.[18]

The system of balance equations taking into account the probabilities obtained above was solved successively for different populations beginning with the lowest levels 6D, 4F, 5G, 6H etc. The calculation was terminated when the relative populations attained equilibrium as determined by Boltzmann's formula. Then successive substitutions (starting from the top) were used to obtain the populations of all levels up to 4F and 6D. The recombination coefficient was determined from

$$dn_e/dt = -N_4(A_{45} + {}^4C_5 n_e) - N_6(A_{66'} + {}^6C_{6'} n_e) = -\alpha n_e^2. \quad (11)$$

Here the subscript 4 pertains to the 4F level, 5 to 5D, 6 to 6D, and 6′ to 6P. The calculated values of α for different n_e and T_e are given in Fig. 3.

The fact that classical cross sections were used naturally limits the accuracy of the results. However, it can be expected that the recombination coefficient does not depend very strongly on the selected form of the cross section.[19] In addition, the error contributes equally to the cross sections for direct and reverse processes, and this is compensated to some extent in the final result.

The recombination coefficients obtained here are in good agreement with recently published calculations of Bates et al.[20] for ions of alkali metals. However, they are up to one order of magnitude larger than the value of α obtained in [7] for helium.

Since for large concentrations the dominant role is played by nonradiative transitions, a considerable fraction of the plasma ionization energy is transformed in collisions of the second kind to kinetic energy of the electron gas. For a plasma decaying purely by recombination the electron energy balance equation is

$$\frac{d}{dt}\left(\frac{3}{2} kT_e n_e\right) = -\Delta W + \bar{\varepsilon} \frac{dn_e}{dt},$$

where ΔW is the energy loss per unit time in collisions of electrons with atoms and ions, and $\bar{\epsilon}$ is the mean kinetic energy liberated in each recombination. Since ϵ can have a value 2—3 eV, the energy liberated in recombinations makes an important contribution to the thermal balance of the electrons by slowing down the decrease of electron temperature. This accounts for the fact that we observed the stabilization of T_e at a relatively high level (Fig. 1) during a millisecond, whereas only electron-ion collisions would cool electrons to room temperature after approximately 200 μsec (in the absence of external heating). Mohler [1] observed the slow cooling of electrons from T_e = 2700° K in an active plasma to 1350° K in 0.9 μsec and to 1200° K in 1.8 μsec after termination of the current.

The author is indebted to Professor V. L. Granovskiĭ for suggesting this research and for his continual interest.

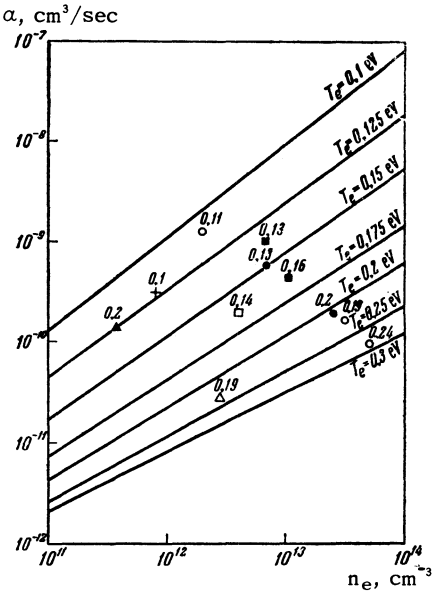

FIG. 3. Recombination coefficient $\alpha(n_e, T_e)$. The continuous curves represent calculations. Experimental results are denoted as follows: + — Mohler[1]; ▲ — D'Angelo and Rynn[3]; Δ — Wada and Knechtli[4]. The remaining points were obtained in the present work: ■ — p = 2.8 × 10⁻², □ — 4.0 × 10⁻², ○ — 0.1 mm. The numbers adjacent to the experimental-value symbols designate the electron temperature in eV.

[1] F. L. Mohler, J. Research Natl. Bur. Standards 19, 447 (1937).

[2] P. Dandurand and R. B. Holt, Phys. Rev. 82, 278 (1951).

[3] N. D'Angelo and N. Rynn, Phys. Fluids 4, 1303 (1961).

[4] J. Y. Wada and R. C. Knechtli, Proc. Inst. Radio Engrs. 49, 1926 (1961).

[5] A. Guthrie and R. K. Wakerling (eds.), The Characteristics of Electrical Discharges in Magnetic Fields, McGraw-Hill, New York, 1949, p. 77.

[6] F. L. Mohler and C. Boeckner, J. Research Nat. Bur. Standards 2, 489 (1929).

[7] E. Hinnov and J. G. Hirschberg, Phys. Rev. 125, 795 (1962).

[8] O. S. Pavlichenko and L. A. Dushin, Optika i spektroskopiya 12, 541 (1962).

[9] Yu. M. Aleskovskiĭ and V. L. Granovskiĭ, JETP 43, 1253 (1962), Soviet Phys. JETP 16, 887 (1963).

[10] L. B. Loeb, Basic Processes of Gaseous Electronics, Univ. of California Press, 1960, p. 590.

[11] F. W. Loomis and P. Kusch, Phys. Rev. 46, 292 (1934).

[12] N. D'Angelo, Phys. Rev. 121, 505 (1961).

[13] D. R. Bates and A. Damgaard, Phil. Trans. Roy. Soc. London A242, 101 (1949).

[14] L. S. Ornstein and J. Key, Z. Physik 85, 565 (1933).

[15] R. W. P. McWhirter, Nature 190, 902 (1961).

[16] D. R. Bates and A. E. Kingston, Nature 189, 652 (1961).

[17] C. W. Allen, Astrophysical Quantities, The Athlone Press, London, 1955, p. 56.

[18] M. I. Petrashen' and I. V. Abarenkov, Vestnik, Leningrad State University, 5, 141 (1954).

[19] Biberman, Toporkin, and Ul'yanov, ZhTF 32, 827 (1962), Soviet Phys.-Tech. Phys. 7, 605 (1963).

[20] Bates, Kingston, and McWhirter, Proc. Roy. Soc. (London) A267, 297 (1962).

Translated by I. Emin
141